Analytical and experimental study on a WEC-type floating breakwater

Dezhi Ning[#1], Xuanlie Zhao[#2], Jun Zang[#*3], Lars Johanning[#&4]

[#]*State Key Laboratory of Coastal and Offshore Engineering, Dalian University of Technology, Dalian, 116024, China*

[1]dzning@dlut.edu.cn

[2]zhaoxuanlie@163.com

[*]*Department of Civil Engineering and Architecture, University of Bath, Bath, BA2 7AY, UK*

[3]j.zang@bath.ac.uk

[&] *College of Engineering, Mathematics and Physical Sciences, University of Exeter, Cornwall TR10 9FE, UK*

[4]l.johanning@exeter.ac.uk

***Abstract*— A dual-pontoon wave energy converter (WEC)-type floating breakwater, which is expected to overcome the shortcomings of the single-pontoon system (i.e., the narrow effective frequency bandwidth for the effective transmission coefficient $K_T < 0.5$ and the qualified capture width ratio CWR $\eta > 20\%$), is proposed. The dual-pontoon system consists of a pair of single-pontoon WEC-type floating breakwaters (details see Ref. [1]). An analytical method based on linear potential flow theory is adopted to predict the hydrodynamic performance of the single-pontoon and dual-pontoon WEC-type floating breakwaters, respectively. Analytical solution showed that the effective frequency bandwidth for the dual-pontoon system is obviously broader than that for the single-pontoon case. Note that, economically, the volume of the dual-pontoon system equals to that of the original single-pontoon system. Furthermore, to confirm the phenomenon of boarder effective frequency bandwidth found by analytical method, an two-dimensional experimental study is conducted to investigate the hydrodynamic performance of the WEC-type floating breakwater. The power take-off (PTO) system consisting of the magnetic powder brake, the current controller and the torque-power sensor is used to measure the produced power and the damping force. Experimental results also reveal that the dual-pontoon system performs more effective than the single-pontoon system in terms of the effective frequency bandwidth.**

***Keywords*—Wave Energy Converter, Breakwater, Effective Frequency Bandwidth, Analytical Study, Experimental Study**

I. INTRODUCTION

As a kind of inexhaustible clean energy, wave energy is attractive for engineers and researchers recently. However, the challenge of high construction-cost may be the obstacle which limits the development of the wave energy utilization [2]. From the point of engineering application, the cost-sharing strategy may decrease the construction-cost effectively. Cost-sharing can be achieved by integrating wave energy devices into other marine structures (such as breakwaters, offshore wind turbine, offshore platform, etc.) [1, 3].

Many attempts have been made with respect to combinations of wave energy converters and breakwaters. The wave energy converters which are expected to be integrated into breakwaters mainly include two categories: Oscillating Water Column (OWC) and floating buoy types. Investigation of integrated system consists of OWC-type WEC and caisson breakwater emerged at an earlier time [4]. Recently, some researchers improve the OWC-type caisson breakwater by introducing the U-OWC concept [5]. It is understood that the floating breakwater is favoured for its advantages of flexibility and environmental friendless. He and Huang [6] integrated the classical OWC-type WEC into the floating breakwater with pneumatic chambers. For the categories of floating buoy-type WECs, Michailides and Angelides [7] proposed a flexible floating breakwater with PTO system installed to capture the kinetic energy of the relative motion of the adjacent modules; Chen et al. [8] used the horizontal floating cylinders as both WECs and floating breakwaters, and the PTO system was installed to capture the kinetic energy of the heave motion of the cylinders; Ning et al. [1] integrated oscillating buoy-type WEC into a pile-restrained floating breakwater, which possesses a favorable property, i.e., form succinctness. Experimental results showed that qualified wave attenuation performance and energy-conversion efficiency can be achieved, with appropriate dimensions and PTO damping setting.

It is understood that the single-pontoon system proposed in Ref. [1] has a narrow effective frequency bandwidth, for which the condition of $K_T < 0.5$ and $\eta < 20\%$ can be realized. Ning et al. [9] introduced an improved arrangement of dual-pontoon WEC-type breakwater with aiming of broadening the effective frequency bandwidth of the integrated systems. In this study, the analytical investigation of single-pontoon system and the dual-pontoon system is conducted. Furthermore, the confirmatory experimental investigation is conducted with focus on the transmission coefficient and the CWR of the single-pontoon system and the dual-pontoon system.

The paper is organized as follows. In section 2, the used analytical method and the experimental setup are described. In section 3, the analytical and experimental results are presented and discussed. In Section 4, the conclusions are given.

II. METHODS

A. Analytical method

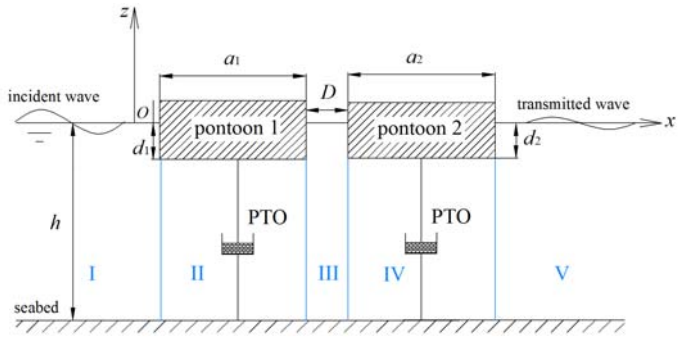

Figure 1 Sketch of the two-dimensional dual-pontoon WEC-type breakwater (pontoon 1 is the front pontoon and pontoon 2 the rear pontoon).

The sketch of the two-dimensional oscillating buoy WEC is shown in Fig. 1. The breadths of the pontoon 1 and pontoon 2 are defined as a_1 and a_2, the drafts d_1 and d_2, respectively, and the spacing between the two pontoons is D. The integrated system with dual floating pontoons is installed in the water with uniform depth h. An analytical model is developed based on linear potential flow theory and matching eigen-function expansion technique. The detailed description of the solution and the calculation of the transmission coefficient K_T, total CWR η (i.e., CWR of pontoon 1 and pontoon 2) and Response Amplitude Operator in Heave mode (HRAO) ζ can obtained from Ref. [9, 10]. Note that the configuration with pontoon 1 moving in heave mode and pontoon 2 fixed can be achieved by setting the stiffness of the second pontoon as infinity. The hydrodynamic problem corresponding to the single-pontoon system can be dealt with by setting the size of pontoon 2 as infinitesimal.

B Experimental setup

The experiments were conducted in a wave flume at the State Key Laboratory of Coastal and Offshore Engineering, Dalian University of Technology, China. The dimensions of the flume are 69 m in length, 2 m in width and 1.8 m in depth. A wall was installed along the longitudinal direction of the wave flume to divide the width of the flume into two parts: 1.2 m width and 0.8 m width, where the part of 0.8 m width was selected as test section. A 1:13 model was adopted to build the experimental model based on Froude scaling. Fig. 2 shows the physical model of the two identical pontoons. For each pontoon, the width, height and transverse length are 0.5 m, 0.6 m and 0.78 m, respectively. Fig. 3 shows a sketch of the experimental setup. The two pontoons were pile-restrained at the test location, which was 45 m away from the wave-maker. Four wave gauges were arranged at the weather and lee sides of the model to record the water surface elevations, respectively, and the two-point method was used to deal with the reelection coefficient and the transmission coefficient [12]. The rear pontoon is moved out of the flume while testing the single-pontoon system. The pontoon was held by two vertical piles, which are located at the upwave and downwave sides of the pontoon. The PTO system consists of a magnetic powder brake and a tension controller. The produced power can be measured by the torque-power sensor. The heave motion of the device can be measured by the displacement sensor. The connections of the device (pontoon 1) with the PTO system and the sliding piles have been described detailly in Ref. [1].

Fig. 2 Physical model of the front pontoon (i.e., pontoon 1) and rear pontoon (i.e., pontoon 2)

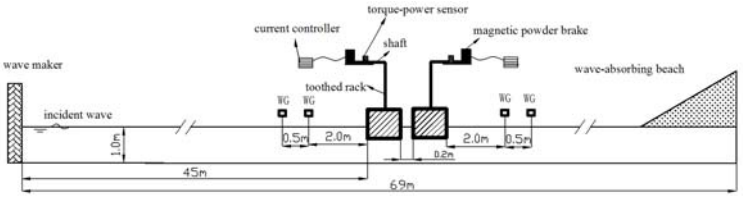

Fig. 3 A sketch of the experimental setup. WG: wave gauge.

The experiments are divided into two stages, i.e., the tests of single-pontoon system and dual-pontoon system. During the whole process, the still water depth was fixed as 1 m. The tested cases for the single-pontoon system can be seen in Tab. Ⅰ. The draft of pontoon is d = 0.25 m and the breadth is a = 0.6 m. The test cases for the dual-pontoon system can be seen in Tab. Ⅱ. The drafts are $d_1 = d_2$ = 0.125 m, and the breadths are $a_1 = a_2$ = 0.6 m, and the distance D = 0.2 m. The test wave periods are chosen based on the sea states in East China Sea and the details (period and wave amplitude) refer to Tab. I and ~~II~~~~III~~ in the Appendix.

III. Results and Discussions

A. Analytical respect

In this section, the hydrodynamics (CWR η and transmission coefficient K_T) of the dual-pontoon system and the single-pontoon system are of interested. Considering that the volume of the offshore structure affects its cost, the total volume of the two pontoons shall be equal to that of the single device. To ensure the equal volumes, the drafts of the dual-pontoon system are fixed as d_1 = 0.125 and d_2/h = 0.125 and the breadths as $a_1/h = a_2/h$ = 0.6. Since the dual-pontoon system with smaller distance D/h results in better energy conversion performance, D/h is chosen as 0.2 in the present study [9]. Note that the optimal damping corresponding to the isolated case is adopted to calculate the produced power for each device (details see Ref. [9]). The draft of the single-pontoon system fixed as d/h = 0.25 and the breadth as a/h =

0.6. For the dual-pontoon system, we consider two scenarios: (1) both the front pontoon and the rear pontoon move in heave mode under control of the PTO system, and (2) the front pontoon moves in heave mode under control of the PTO system and the rear pontoon is fixed. For convenience, we named the former scenario as Scenario 1, the latter one as Scenario 2. Scenario 3 corresponds to the single-pontoon system.

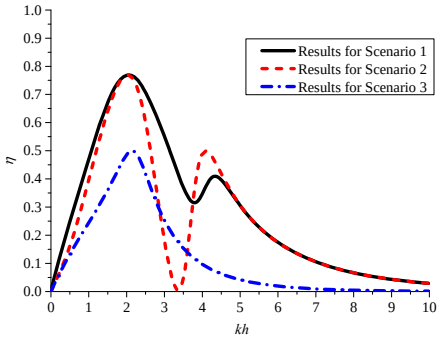

Figure 4 Variations of the CWR η *vs.* the dimensionless wavenumber kh for Scenario 1, 2 and 3.

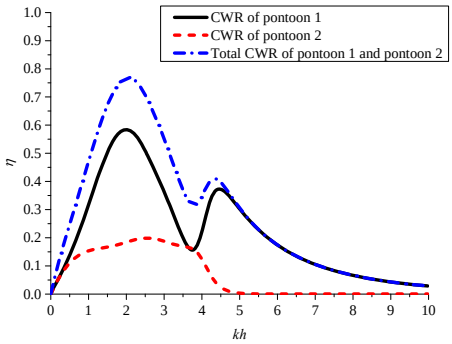

Figure 5 Variations of the CWR η *vs.* the dimensionless wavenumber kh for the front pontoon, rear pontoon and the total CWR of Scenario 1.

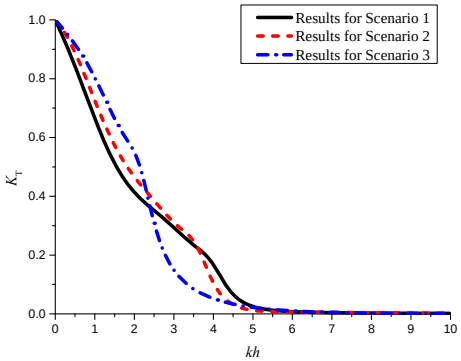

Figure 6 Variations of the transmission coefficient K_T *vs.* the dimensionless wavenumber kh for Scenario 1, 2 and 3.

Fig. 4 presents the variations of η *vs.* kh for Scenario 1, 2 and 3. It can be seen that the CWR of the dual-pontoon systems (Scenario 1 and 2) is remarkedly greater than that of the single-pontoon system at the most frequency region, with exception of the frequency region corresponding to the zero value of the CWR for Scenario 2. The standing waves formed in front of a fixed structure may lead to the phenomenon of the zero value of CWR for Scenario 2. This may result in that the CWR for Scenario 2 is significantly smaller than that for Scenario 1 at region of kh=2.5~3.7, approximately. Fig. 5 shows the results of CWRs for the front pontoon and rear pontoon and the total CWR in the case of Scenario 1. The CWR of the rear pontoon is much smaller than that of the front pontoon due to the shadowing effect. Specially, the CWR of the rear pontoon approaches to zero for region of kh > 5. Since this phenomenon occurs at the high frequency region, it may not make practical significance from the point of engineering application.

Fig. 6 gives the variations of K_T *vs.* kh for Scenario 1, 2 and 3. At the lower frequency region (kh < 2.4), the transmission coefficient at Scenario 1 is smaller than that at Scenario 2. And the wave attenuation performance of the single-pontoon system performs the worst among three scenarios. But a better wave attenuation performance for the single-pontoon system is shown at region of 2.4< kh < 4.5. The transmission coefficient approaches to zero for the three scenarios at high frequency regions (i.e., kh > 5).

From the above results, it can be seen that the effective frequency bandwidth (i.e., K_T < 0.5 and η > 20%) of the dual pontoon system is markedly broader than that of the single-pontoon system.

B. Experimental aspect

The analytical study is conducted in frequency domain, which leads to the linearity of the relating physical quantities. Furthermore, the friction loss and the viscous effect are not considered. Thus, the experimental study is conducted to confirm the analytical conclusion.

1) Comparison between the experiment and theory

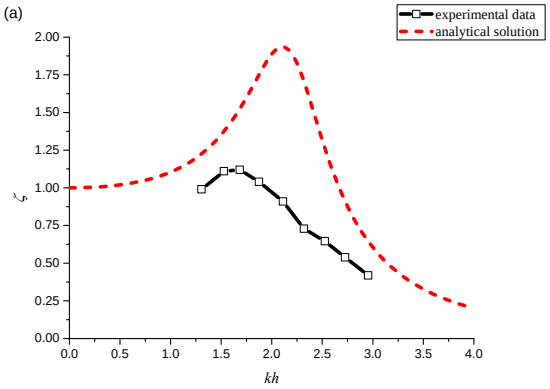

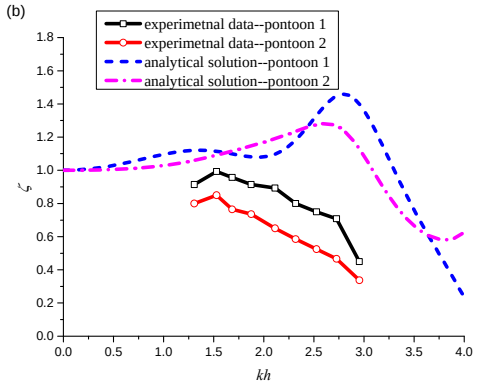

Figure 7 Comparison of HRAO ζ between the experimental data and the analytical solutions for the single-pontoon system (*a*) and dual-pontoon system with Scenario 1 (*b*).

To verify the experiment design, the cases with zero exciting current were carried out. Two groups are considered: 1) single-pontoon system (Scenario 3) with parameters of d = 0.25 m and a = 0.6 m, and 2) dual-pontoon system (Scenario 1) with parameters of $d_1 = d_2 = 0.125$ m, $a_1 = a_2 = 0.6$ m and D = 0.2 m. The test cases for single-pontoon system and dual-pontoon system are shown in Tab. IV~~I~~ and V~~I~~VI~~I~~ (case 1), respectively. Fig. 7(a) and (b) show the comparisons of the experimental and analytical results of HRAO ζ for the single-pontoon system and dual-pontoon system, respectively. It can be seen that the HRAO ζ from the two methods presents similar trends. However, the *kh* corresponding to peak value of ζ in the experiment is not totally consistent with the analytical solutions. This may be due to the fact that the mass of the power take-off system is not considered in the analytical analysis. Furthermore, the viscous effect and the friction in the transmission mechanism are also not included, which may lead to the HRAO in the experiment smaller than that of the analytical solutions. Therefore, the difference between the two results can be expected. Nevertheless, the overall variation trend between them verifies the experimental design.

2) Experimental results

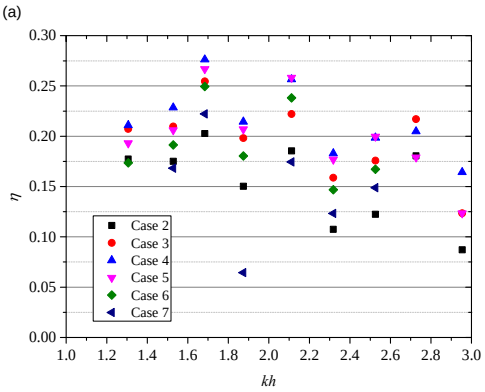

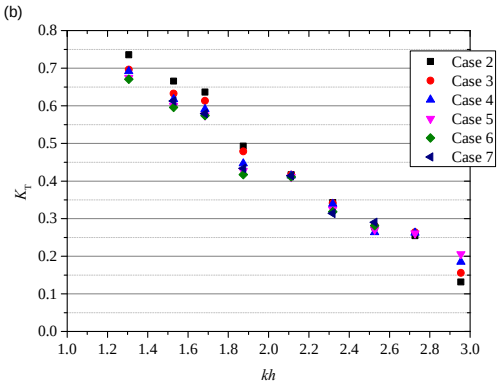

Figure 8 Variations of η *vs.* F_{PTO} (a) and K_T *vs.* F_{PTO} (b) with different wavenumber for the single-pontoon system (d = 0.25 m and a = 0.6 m). (F_{PTO} denotes the PTO damping force acted on the device, and the corresponding F_{PTO} acting on the device refers to Tab. VII~~I~~)

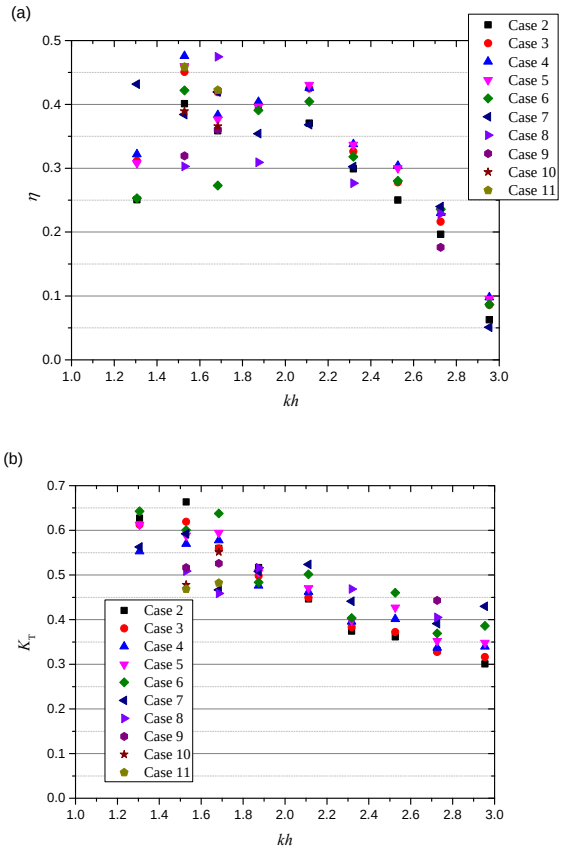

Figure 9 Variations of η *vs.* F_{PTO} (a) and K_T *vs.* F_{PTO} (b) with different wavenumber for the dual-pontoon system ($d_1 = d_2$ = 0.25 m and $a_1 = a_2$= 0.6 m). (The corresponding F_{PTO} acting on the device refer to Tab. VIII~~I~~IX~~I~~)

Figs. 8 (a) and (b) show the variations of η vs. F_{PTO} and K_T *vs.* F_{PTO} with the dimensionless wavenumber for the single-pontoon system. It can be seen that the CWR increases firstly and then decreases with the increase of the PTO damping force. The condition for $K_T < 0.5$ and $\eta > 20\%$ can be satisfied by adjusting the F_{PTO} properly for $1.874 < kh < 2.726$ with the exception of kh = 2.318. For the frequency region of kh <

1.874, the proposed condition cannot be satisfied due to the transmission coefficient greater than 0.5. Figs. 9 (a) and (b) show the variations of η vs. F_{PTO} and K_T *vs*. F_{PTO} with dimensionless wavenumber for the dual-pontoon system. It can be seen that the condition for $K_T < 0.5$ and $\eta > 20\%$ can be satisfied by adjusting the F_{PTO} properly for $1.528 < kh < 2.726$. That is to say, the effective frequency bandwidth of the dual-pontoon system is broader than that of the single-pontoon system with equal volume. Note that the transmission coefficient of the dual-pontoon system with the configuration at Scenario 2 is greater than that at Scenario 3.

C. Discussions

From the physical experiment and the analytical analysis, it can be concluded that the effective frequency bandwidth can be broadened by introducing the dual-pontoon system. It is worthy to note that the total volume of the dual-pontoon system equals to that of the original single-pontoon system. In terms of wave attenuation performance, the dual-pontoon system at Scenario 1 (both two pontoons work as WECs) performs better than that at Scenario 2 (only the front pontoon worked as WEC and the rear pontoon is fixed) in longer waves. Only few cases are tested for the dual-pontoons system at Scenario 2. The further optimization is necessary to achieve the optimal wave attenuation performance and CWR.

Since only one PTO system is needed, Scenario 2 is favourable in terms of the cost. However, the worse wave attenuation performance in longer waves may be the shortcoming. Installing a horizontal plate under the rear pontoon may improve the wave attenuation performance of a pontoon type breakwater for the long waves [11]. Thus, it is worthy to investigate the performance of the integrated system by introducing a horizontal plate.

IV. Conclusions

The hydrodynamic properties of the single-pontoon and the dual-pontoon WEC-type breakwater have been investigated analytically and experimentally. The dual-pontoon system includes two scenarios: 1) both the front and rear pontoons work as the WEC, i.e., Scenario 1, and 2) the front pontoon works as the WEC and the rear pontoon is fixed i.e., Scenario 2. In the analytical study, the absorbed power is calculated by using the linear PTO damping, which corresponds to the isolated case. The total volume of the dual-pontoon system is equal to the volume of the single-pontoon system. The comparisons between the single-pontoon system and the dual-pontoon system are conducted. Furthermore, the experimental investigation is conducted to verify the conclusion obtained in the analytical study. The PTO system consisting of a magnetic powder brake and a tension controller is used in the experimental study. The conclusions are summarized as follows.

The phenomenon that the dual-pontoon system possesses broader effective frequency bandwidth with the condition of $K_T < 0.5$ and $\eta > 20$ % is revealed analytically. The dual-pontoon system with both pontoons as WECs performs better for the long waves.

Experimental data verifies the conclusion obtained in the analytical study.

Integrated system with one PTO system (i.e., Scenario 2) may be favourable in terms of the cost. However, the shortcoming is that the wave attenuation performance is not qualified for the long waves. To improve the performance of the system for the long wave is worthy to investigate.

Acknowledgment

The authors would like to acknowledge the financial support the National Natural Science Foundation of China (Grant Nos. 51379037 and 51679036) and the Royal Academy of Engineering under the UK-China Industry Academia Partnership Programme (Grant No.UK-CIAPP\73).

References

[1] Ning D, Zhao X, Göteman M, Kang H. Hydrodynamic performance of a pile-restrained WEC-type floating breakwater: An experimental study. RENEW ENERG. 2016; 95:531-541.

[2] Ferro BD. Wave and tidal energy: its emergence and the challenges it faces. Refocus. 2006; 7:46-48.

[3] Bozo NT. A review and comparison of offshore floating concepts with combined wind-wave energy. 2015. p.

[4] Takahashi S, "Hydrodynamic characteristics of wave-power-extracting caisson breakwater," in Twenty-First Coastal Engineering Conference, pp. 2489-2503.

[5] Arena F, Laface V, Malara G, Strati FM, Soares CG, "Optimal configuration of a U-OWC wave energy converter," in 1st International Conference on Renewable Energies Offshore, RENEW 2014, (CRC Press/Balkema, 2015), pp. 429-436.

[6] He F, Huang Z, Wing-Keung Law A. Hydrodynamic performance of a rectangular floating breakwater with and without pneumatic chambers: An experimental study. OCEAN ENG. 2012; 51:16-27.

[7] Michailides C, Angelides DC. Modeling of energy extraction and behavior of a Flexible Floating Breakwater. APPL OCEAN RES. 2012.

[8] Chen B, Ning D, Liu C, Greated CA, Kang H. Wave energy extraction by horizontal floating cylinders perpendicular to wave propagation. OCEAN ENG. 2016; 121:112-122.

[9] Ning D, Zhao X, Zhao M, Hann M, Kang H. Analytical investigation of hydrodynamic performance of a dual pontoon WEC-type breakwater. APPL OCEAN RES. 2017, 65:102-111.

[10] Zheng S, Zhang Y. Wave diffraction and radiation by multiple rectangular floaters. J HYDRAUL RES. 2016; 54:102-115.

[11] Wang YX, Dong HY, Liu C. Experimental study of a pile-restrained floating breakwater constructed of pontoon and plates. CHINA OCEAN ENG. 2010; 24:183-190.

[12] Goda Y, Suzuki Y. Estimation of incident and reflected waves in random wave experiments. IN: PROC. FIFTEENTH COASTAL ENGNG. CONF. pp. 1828-1977.

TABLE X~~I~~

TEST CONDITIONS FOR THE SINGLE-PONTOON SYSTEM WITH $d = 0.25\ m$ AND $a = 0.60\ m$, T DENOTES THE WAVE PERIOD, A THE INCIDENT WAVE AMPLITUDE, F_{PTO} THE CORRESPONDING TIME-AVERAGED PTO DAMPING FORCE, kh THE DIMENSIONLESS WAVENUMBER (SIMILARLY HEREINAFTER).

	***T* (s)**	**1.17**	**1.22**	**1.27**	**1.33**	**1.4**	**1.5**	**1.6**	**1.7**	**1.89**
	***A* (m)**	**0.04**	**0.06**	**0.06**	**0.07**	**0.07**	**0.07**	**0.07**	**0.07**	**0.07**
	kh	**2.954**	**2.726**	**2.526**	**2.318**	**2.112**	**1.874**	**1.684**	**1.528**	**1.306**
F_{PTO} (N)	Case 1	3.49	3.81	3.31	3.46	3.72	3.92	3.78	3.81	3.84
	Case 2	7.462	23.42	14.06	14.36	25.00	20.7	31.45	31.47	44.48
	Case 3	11.72	33.32	23.06	24.5	32.84	31.03	43.96	41.36	65.08
	Case 4	21.22	42.07	32.36	33.81	43.28	44.27	52.84	60.75	73.05
	Case 5	25.62	47.61	40.20	42.63	53.13	51.59	66.88	77.90	84.56
	Case 6	-	-	45.35	51.79	61.52	59.49	76.88	83.31	99.04
	Case 7	-	-	51.12	56.83	69.86	80.1	84.4	90.99	-

TABLE X~~I~~I~~I~~

TEST CONDITIONS FOR THE DUAL-PONTOON SYSTEM WITH $a_1 = a_2 = 0.6\ m$, $d_1 = d_2 = 0.125\ m$ AND $D = 0.2\ m$. IF ONLY ONE FORCE FPTO IS PRESENTED FOR ONE CASE, IT MEANS THAT THE FORCE IS ACTED ON THE FRONT PONTOON AND THE REAR PONTOON IS FIXED; THE FORM OF a/b THAT THE FORCE a IS ACTED ON PONTOON 1 AND b ON PONTOON 2.

	***T* (s)**	**1.17**	**1.22**	**1.27**	**1.33**	**1.4**	**1.5**	**1.6**	**1.7**	**1.89**
	***A* (m)**	**0.04**	**0.06**	**0.06**	**0.07**	**0.07**	**0.07**	**0.07**	**0.07**	**0.07**
	kh	**2.954**	**2.726**	**2.526**	**2.318**	**2.112**	**1.874**	**1.684**	**1.528**	**1.306**
F_{PTO} (N)	Case 1	3.21/3.45	3.42/3.56	3.46/3.69	3.55/4.10	3.68/3.76	3.90/4.00	3.82/3.96	3.80/4.03	4.05/4.20
	Case 2	9.92	33.04	39.87	50.12	60.83	57.56	59.66	58.88	61.02
	Case 3	16.39	37.62	49.05	60.93	72.88	71.62	82.42	81.38	84.87
	Case 4	20.42	40.78	61.22	69.26	87.45	79.18	105.03	99.34	106.22
	Case 5	23.02	46.78	71.069	71.77	92.86	81.34	121.65	105.12	125.32
	Case 6	30.72	54.66	83.28	80.20	104.55	93.85	140.37	123.26	135.82
	Case 7	54.93	65.06	-	95.56	116.28	105.14	99.80/38.33	136.89	114.4/45.10
	Case 8	-	69.87	-	106.77	-	107.47	101.80/43.29	99.91/20.40	-
	Case 9	-	79.55	-	-	-	-	112.03/27.84	103.12/26.68	-
	Case 10	-	-	-	-	-	-	92.28/13.22	99.11/33.99	-
	Case 11	-	-	-	-	-	-	94.31/26.87	99.08/48.90	-